EAS 8803 - Obs Seismology
Lec#13: Array Analysis

- Dr. Zhigang Peng, Spring 2019

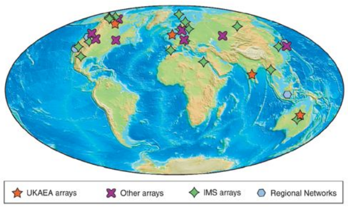

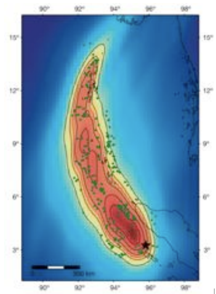

Last Time

- Stacking in exploration geophysics
- Stacking to obtain reliable deep Earth structure
- Stacking to estimate seismic source properties

This Time

- Data management and basic data processing tools
- Systematic and random errors
- Waveform stacking
- Array analysis

Array Analysis

- Introduction of array
- Basic array processing techniques
- Example of array processing techniques for Earth structures
- Example of array processing techniques for earthquake source properties

Definition

- Seismic array: many uniform seismometers in a well-defined, closely-spaced configuration (*Rost and Thomas*, Rev. Geophys., 2002).
- *Rost and Garnero* (EOS, 2004) gave the following criteria for seismic array:
  - Three or more seismometers
  - An aperture of more than 1 and and less than a few hundred kms
  - Uniform instrumentation and recording
  - A means of analysis of the data as an ensemble
  - A common time signal.

Definition

- Array processing techniques: methods of using the abilities of seismic arrays to measure the vector velocities of an incident wavefront, i.e., slowness and back azimuth.
- Difference between global and regional seismic network: more focused in the purpose, more strict in their configuration, and different analysis tools.

Figure 6.6-16: Station map of the Federation of Digital Broad-Band Seismographic Networks (FDSN).

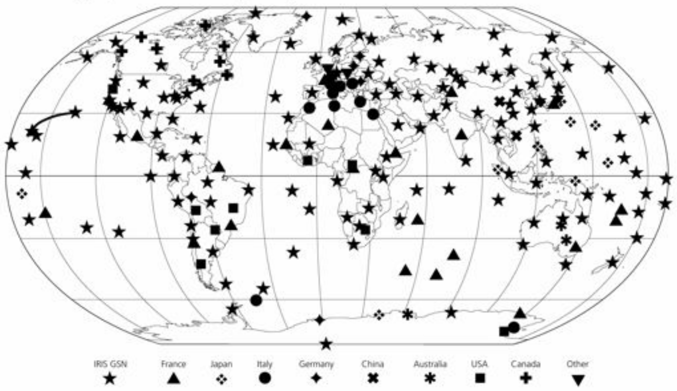

Figure 6.6-18: Map of regional network seismometers in the continental USA.

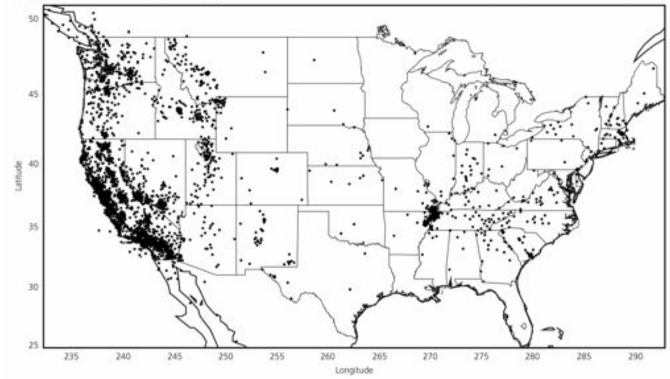

Figure 6.6-17: Station geometry of the Large Aperture Seismic Array (LASA).

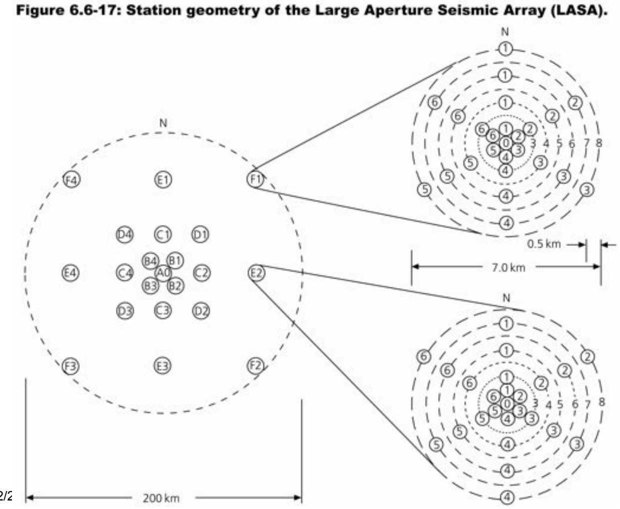

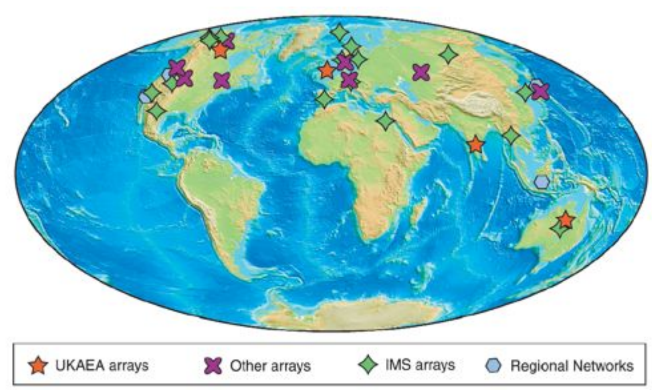

Why should we use arrays?

- This information can be used to distinguish between different seismic phases, separate waves from different seismic events and improve the signal-to-noise ratio by stacking with respect to the varying slowness of different phases.
- The vector velocity information of scattered or reflected phases can be used to determine the region of the Earth from whence the seismic energy comes and with what structures it interacted.

Why should we use arrays?

- Therefore seismic arrays are perfectly suited to study the fine-scale structure and spatio-temporal variations of the material properties of the Earth's interior.
- Array analysis can also be used to better quantify the seismic source mechanisms (e.g., rupture duration, velocity, areas, etc), and forensic seismology (Nuke detection, terrorist attacks, etc).

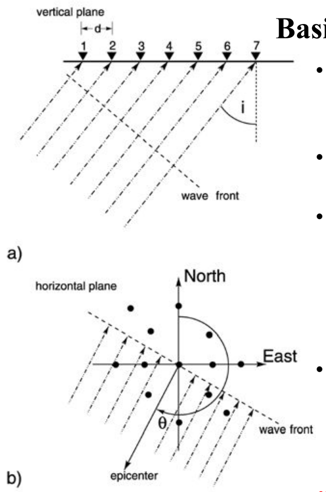

Basics of Array Analysis (AA)

- Most array analysis methods assume a plane wave arriving at the array.
- This is a good approximation for teleseismic events.
- The propagation of an elastic waves can be described by two parameters:
  - Vertical incident angle i,
  - Back azimuth θ.
- In practice, we often use the inverse of the apparent velocity of the wavefront $1/V_{app}$

$$u = \frac{1}{V_{app}} = \frac{\sin i}{V_0}$$

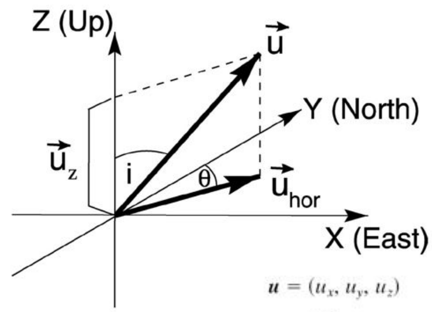

Figure 2. Components of the slo nents incident angle i and back az are marked. The slowness vector is front.

$$\mathbf{u} = (u_x, u_y, u_z)$$

$$= \left(\frac{\sin\theta}{v_{app}}, \frac{\cos\theta}{v_{app}}, \frac{1}{v_{app}\tan i}\right)$$

$$= u_{hor}\left(\sin\theta, \cos\theta, \frac{1}{\tan i}\right)$$

$$= \frac{1}{v_0}(\sin i\,\sin\theta, \sin i\,\cos\theta, \cos i). \qquad (2)$$

A the surface:

$$p = \frac{r_0}{v_0 \sin i} = r_0 u$$

At the bottoming depth, $r = r_p$, and

$$p = \frac{r_p}{v_p}$$

Figure 3.4-2: Geometry of a ray path in a spherical earth.

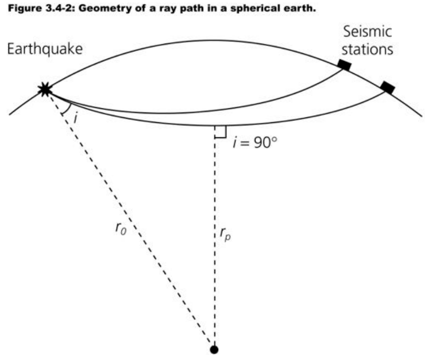

The slowness $\boldsymbol{u}$ is a way to identify different phases traveling through the Earth's interior as it is unique to a given phase in a one-dimensional Earth.

Beam forming

- An important use of seismic arrays is the separation of coherent signals and noise. The basic method to separate coherent and incoherent parts of the recorded signal is array beam forming.
- Beam forming uses the differential travel times of the plane wave front due to a specific slowness and back azimuth to individual array stations.
- If the single-station recordings are appropriately shifted in time for a certain back azimuth and slowness, all signals with the matching back azimuth and slowness will sum constructively.

Station Geometry

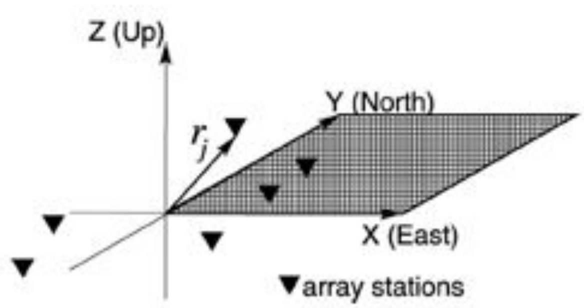

Figure 3. The definition of the sensor position vectors $\mathbf{r}_j$. The center of the array is assumed to be in the center of the Cartesian coordinate system.

Delay and Sum

The incident wavefield at the array center

$$x_{center}(t) = f(t) + n_i(t).$$

Station i with the location r_i records the time series:

$$x_i(t) = f(t - \mathbf{r}_i \cdot \mathbf{u}_{hor}) + n_i(t)$$

with r_i representing the location vector of station i and u_{hor} representing the horizontal slowness vector.

$$\tilde{x}_i(t) = x_i(t + \mathbf{r}_i \cdot \mathbf{u}_{hor}) = f(t) + n_i(t + \mathbf{r}_i \cdot \mathbf{u}_{hor}).$$

The "delay and sum" beam trace for an array with M components is then computed by

$$b(t) = \frac{1}{M}\sum_{i=1}^{M}\tilde{x}_i(t) = f(t) + \frac{1}{M}\sum_{i=1}^{M} n_i(t + \mathbf{r}_i \cdot \mathbf{u}_{hor}).$$

Example of plain sum and "delay and sum"

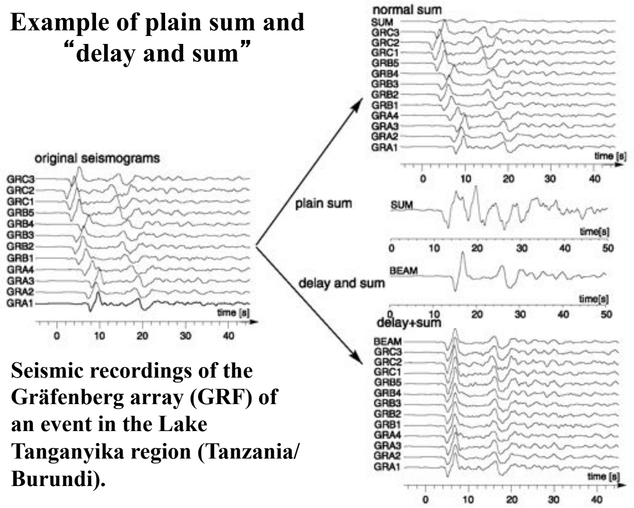

Seismic recordings of the Gräfenberg array (GRF) of an event in the Lake Tanganyika region (Tanzania/ Burundi).

Figure 3.3-23: Illustration of slant stacking.

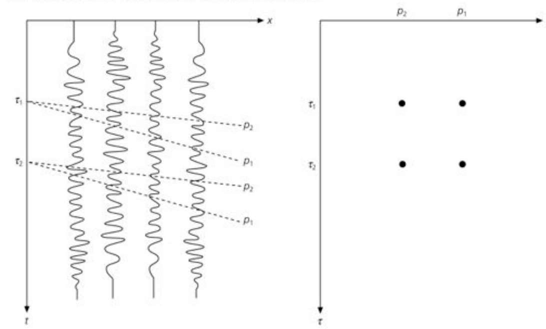

$$\bar{u}(\tau, p) = \int_{-\infty}^{\infty} u(x, \tau + px)dx$$

This integral (*slant stack*) maps all the data along each slanted line in (x, t) to a point in (τ, p).

Vespa Process–Slant Stacks

- The beam forming method enhances the amplitude of a signal with a given slowness ***u***.
- To determine the unknown horizontal slowness or the back azimuth of an arriving signal, the so-called vespa process (velocity spectral analysis [*Davies et al.*, 1971]) can be used.
- The vespa in its original form [*Davies et al.*, 1971] estimates the seismic energy arriving at the array for a given back azimuth and different horizontal slownesses ***u***.
- Alternatively, the vespa process can be used for a fixed slowness and varying back azimuths.
- The result of the vespa process is displayed as a vespagram, a diagram of the energy content (amplitudes) of the incoming signals as a function of slowness or back azimuth and time.

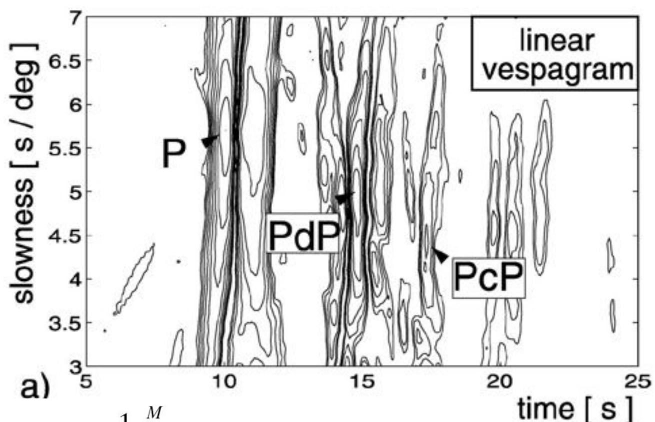

$$v_u(t) = \frac{1}{M}\sum_{i=1}^{M} x_i(t - t_{u,i}),$$

$$g = \frac{\pi \ 6371 \text{ km}}{180°} \cong 111.91 \text{ km/°}.$$

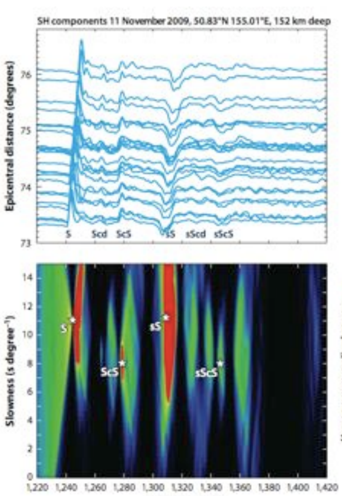

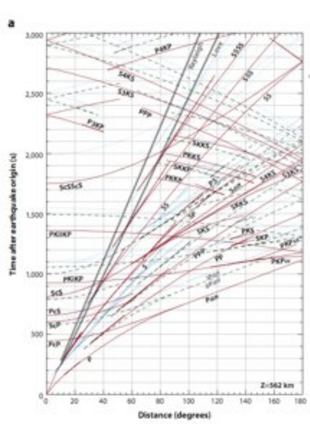

Lay and Garnero (AREPS, 2011)

A wrong back azimuth (slowness) used for the computation may produce misleading slowness (back azimuth) measurements.

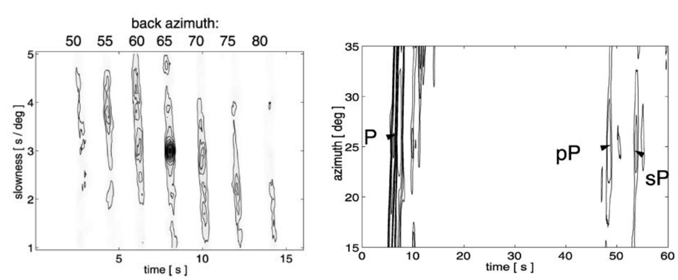

Frequency-wave number analysis

- In contrast to the array methods previously introduced, the frequency-wave number analysis (fk analysis) can measure the complete slowness vector (i.e., back azimuth θ and horizontal slowness u) simultaneously.
- A grid search for all u and θ combinations can be performed to find the best parameter combination, producing the highest amplitudes of the summed signal.

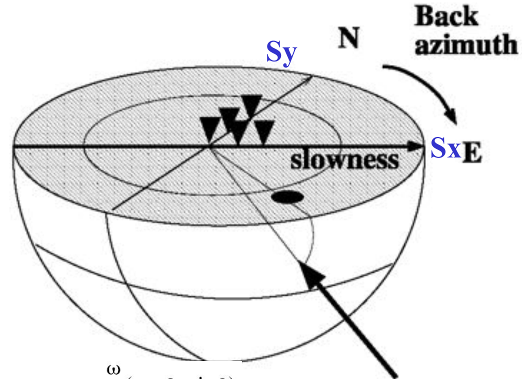

$$\mathbf{k} = (k_x, k_y) = \omega \cdot \mathbf{u} = \frac{\omega}{v_0}(\cos\theta, \sin\theta)$$

$$v_{app} = 1/u_{hor} = \frac{1}{\sqrt{s_x^2 + s_y^2}} \qquad \theta = \tan^{-1}\left(\frac{s_x}{s_y}\right)$$

Three-component Array Processing Techniques

40, 3 / REVIEWS OF GEOPHYSICS ROST AND THOMAS: ARRAY SEISMOL

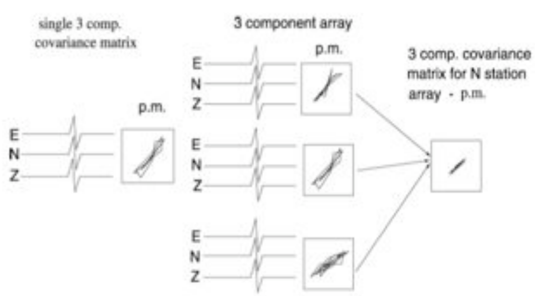

Figure 18. The principle using a three-component array for particle motion studies. For a single three-component station the covariance matrix describes the characteristics of the particle motion. For an array of three-component stations the mean of the covariance matrices of all stations is calculated. The resulting particle motion shows a smaller variance than the individual stations, and the characteristics of the motion as described in the text can be determined with smaller errors.

Array design principle

- Depending on the application of the array (detection, frequency of interest), their geometries vary significantly.
- Design principle:
  - The ARF should have a sharp main lobe, ideally a delta pulse with a strong suppression of the energy next to the main lobe.
  - The sidelobes due to spatial aliasing should not be within the wave number window of interest.
  - The aperture of the array affects the sharpness of the main lobe, i.e., the resolution of the array.
  - The interstation spacing defines the position of the sidelobes in the ARF and the largest resolvable wave number; that is, the smaller the interstation spacing, the larger the wavelength of a resolvable seismic phase will be.

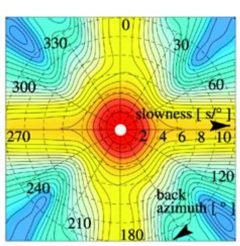

a)

Array response function (ARF) of the small-aperture Yellowknife array (YKA) in northern Canada.

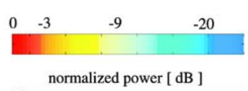

b)

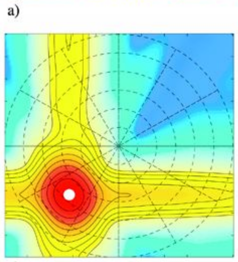

c)

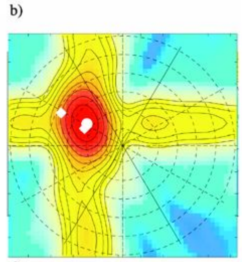

d)

Array response function of GRF.

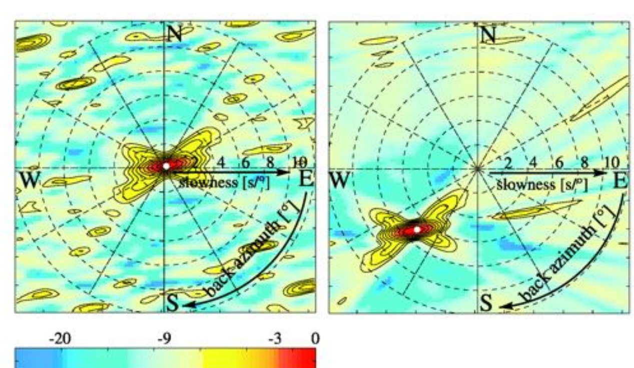

a) b)

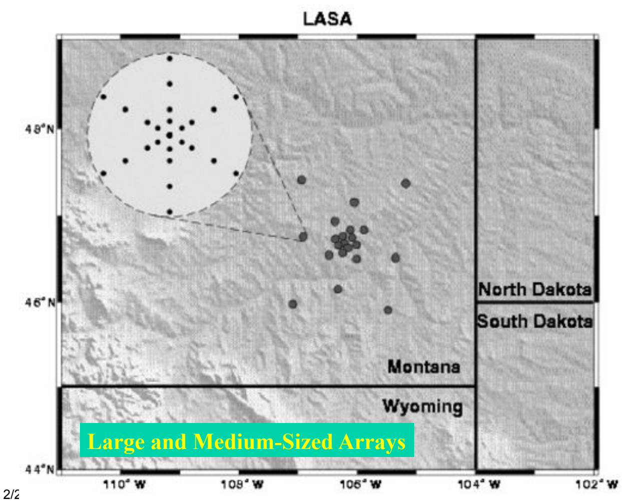

Large and Medium-Sized Arrays

Small Arrays

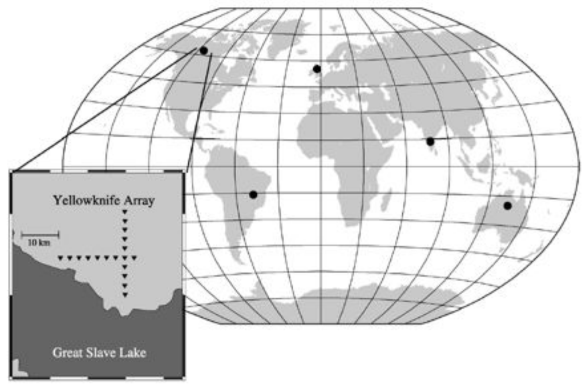

Figure 21. Location of the U.K. Atomic Energy Administration type of array. The arrays are EKA (Eskdalemuir, Scotland), GBA (Gauribidanur, India), WRA (Warramunga, Australia), BDF (Brasilia), and YKA (Yellowknife, Canada). The inset shows the configuration of the Canadian Yellowknife array.

Networks as an array

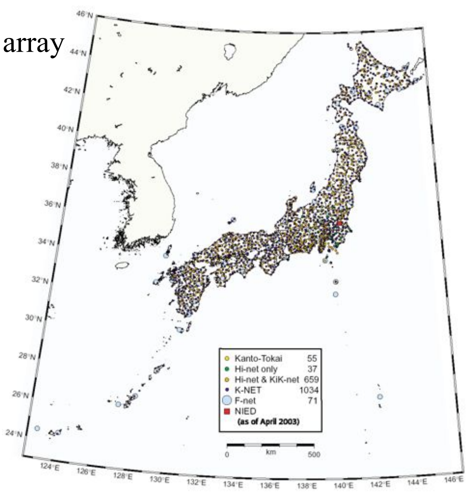

US Array

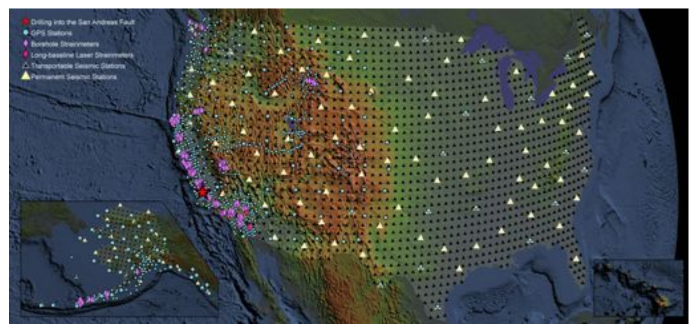

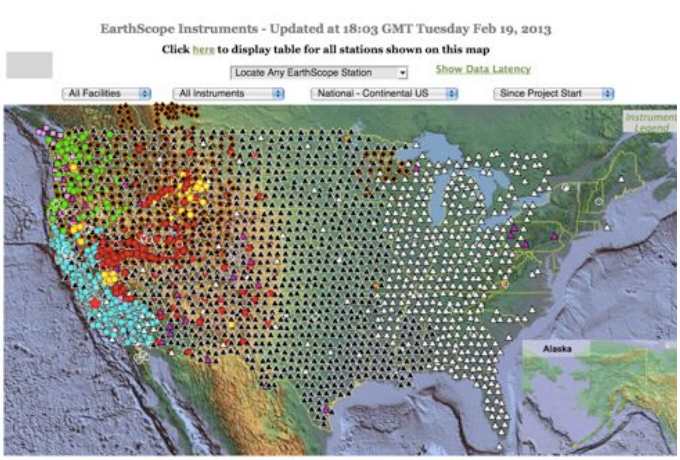

Figure 6.6-17: Station geometry of the Large Aperture Seismic Array (LASA).

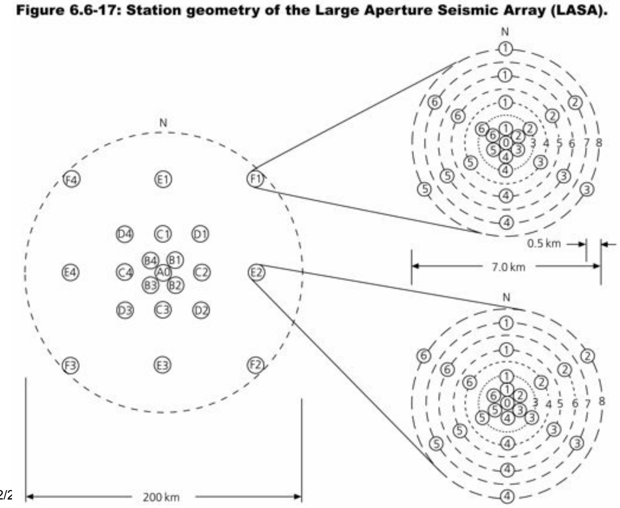

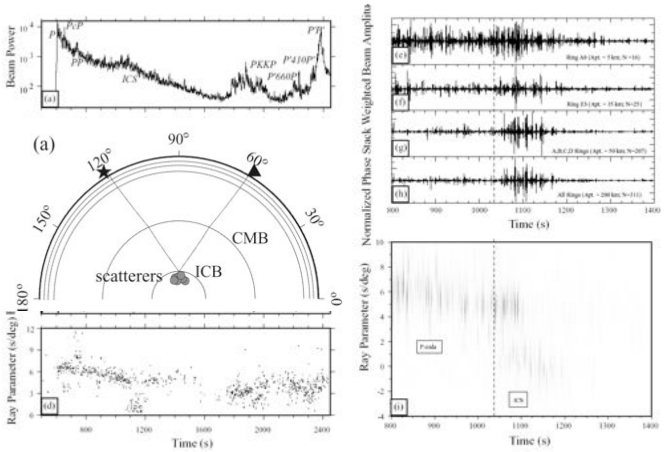

Peng et al. (JGR, 2008)

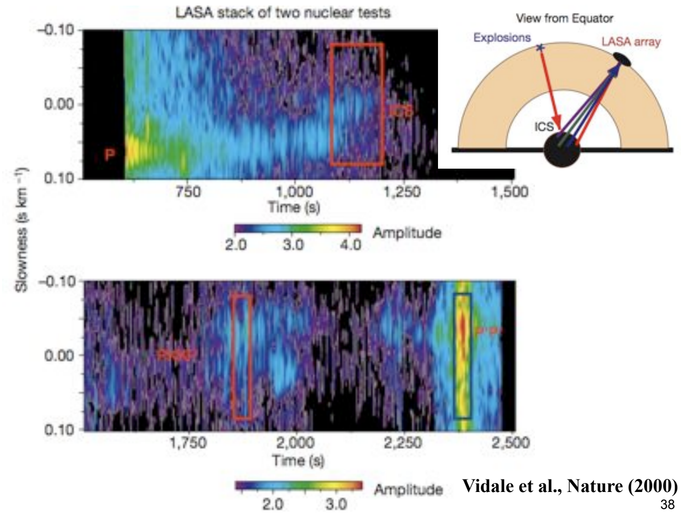

Vidale et al., Nature (2000)

Backpropagation imaging of the 2004 Sumatra earthquake (Ishii et al., Nature, 2005)

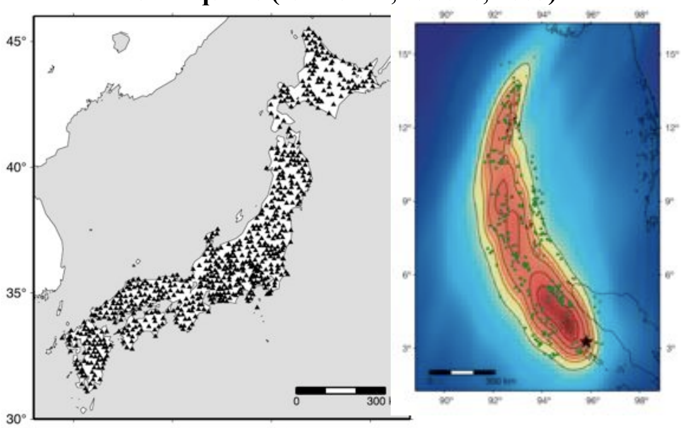

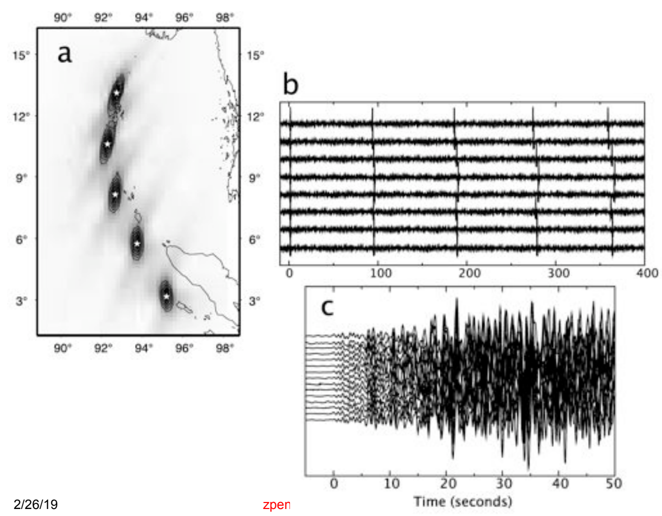

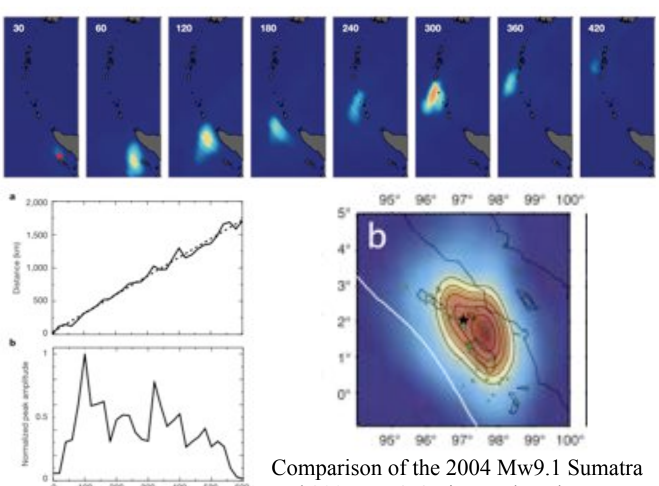

Comparison of the 2004 Mw9.1 Sumatra and 2005 Mw8.6 Nias earthquake

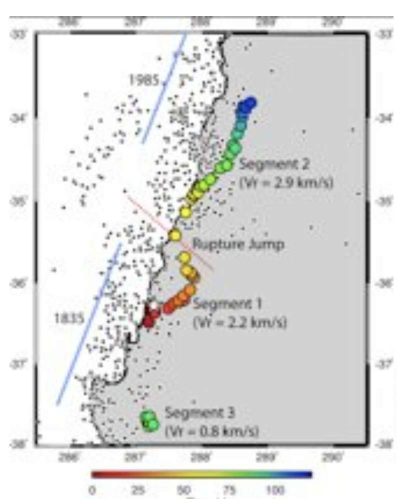

Backprojection of the rupture process for the 2010 Mw8.8 Chile earthquake (Keiser and Ishii, GRL, 2011)

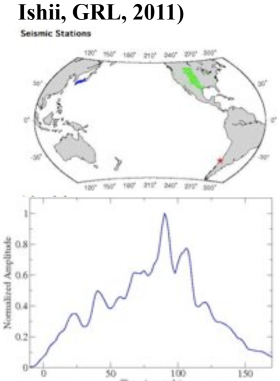

Discrepancy between the finite-fault modeling (long-period) and back-projection results (short-period) [Lay et al., JGR, 2012]

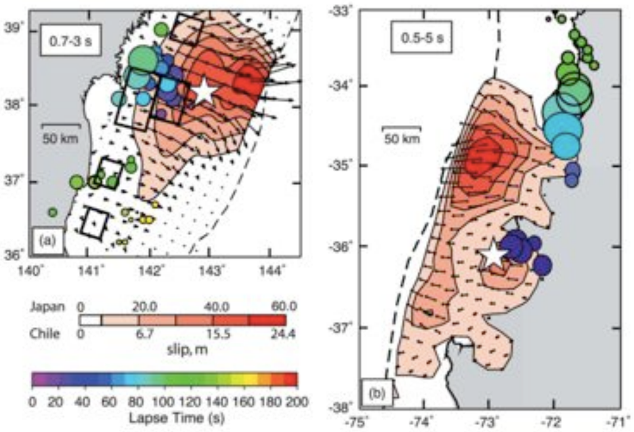

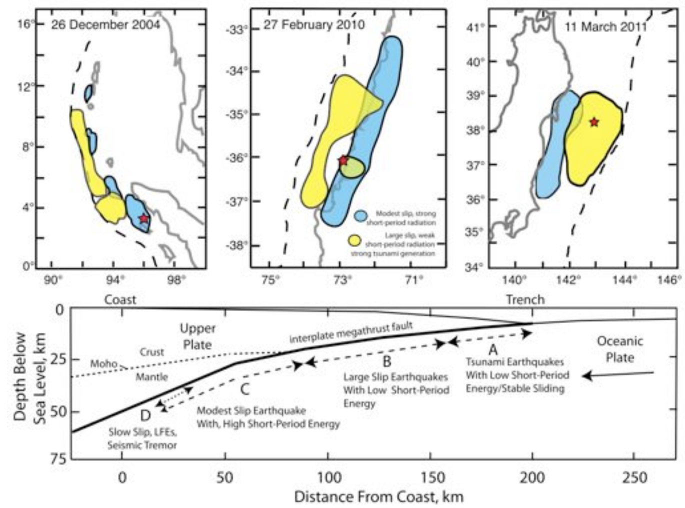

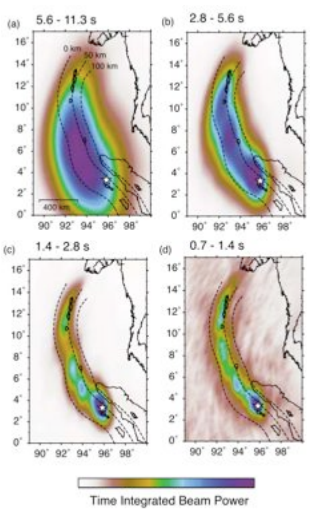

Back-projected P wave beams of the 2004 Mw9.2 Sumatra earthquake with different data and frequency bands

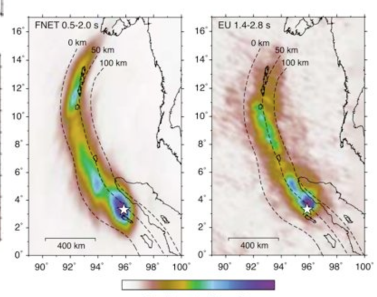

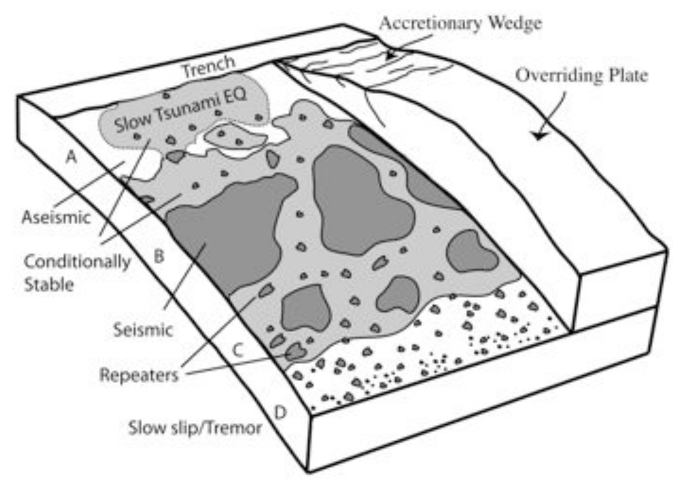

Array of arrays in Cascadia (Ghosh et al., JGR, 2012)

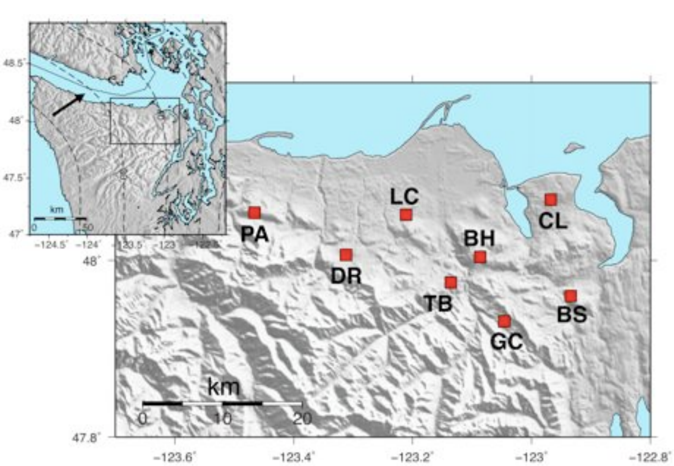

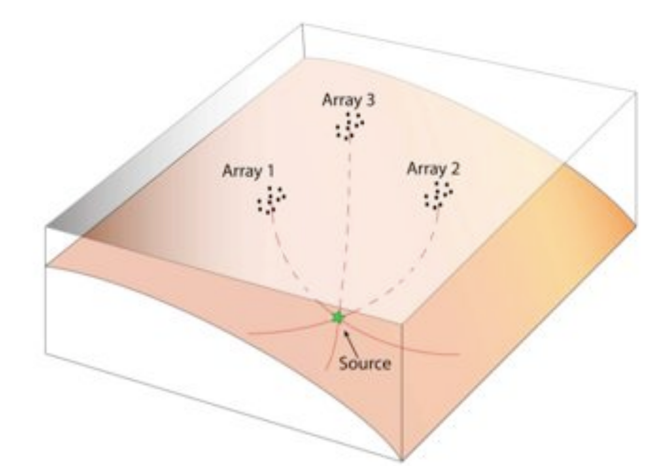

A wide range of tremor behaviors detected by array technique (Ghosh et al., G3, 2010)

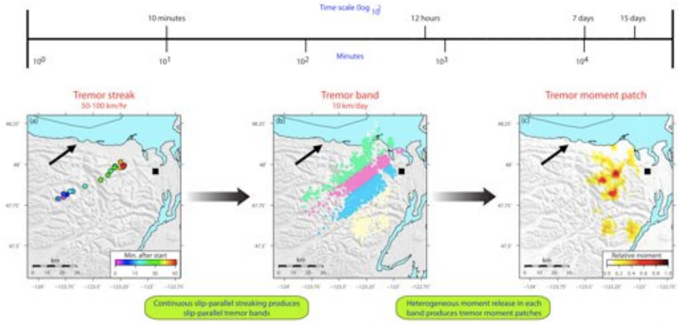

Figure 8. A unified view of tremor distribution in time and space: a time scale ($\log_{10}$) is shown at the top; time increases left to right. The maps show different elements of spatiotemporal tremor distribution observed over different time scales. Positions of the maps along the time scale approximately correspond to the time scales over which these

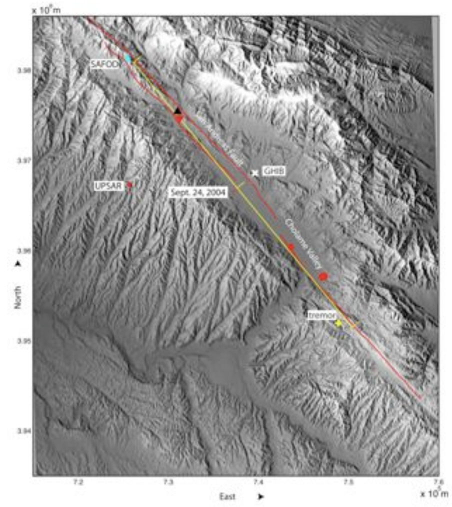

Tremor recorded by the USGS Parkfield Seismic Array (UPSAR) [Fletcher and Baker, JGR, 2010]

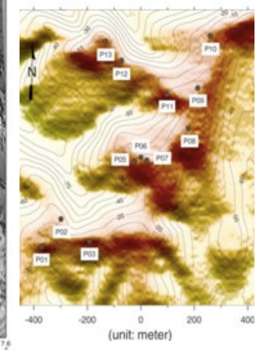

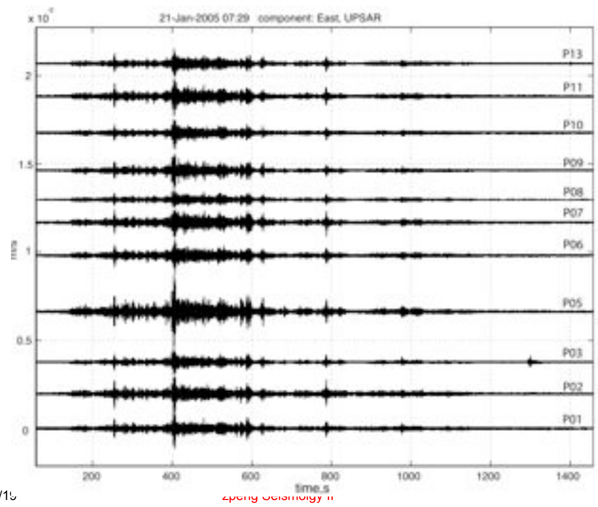

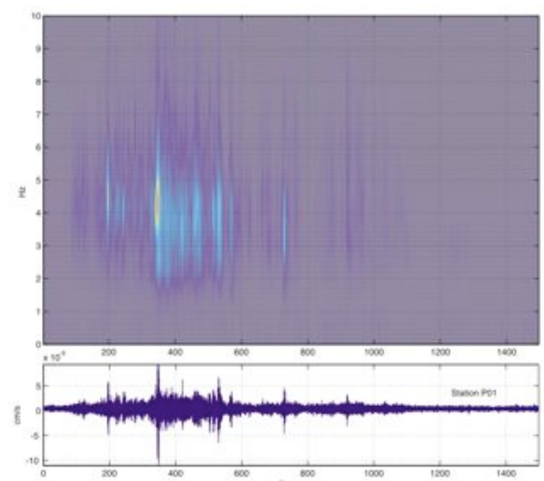

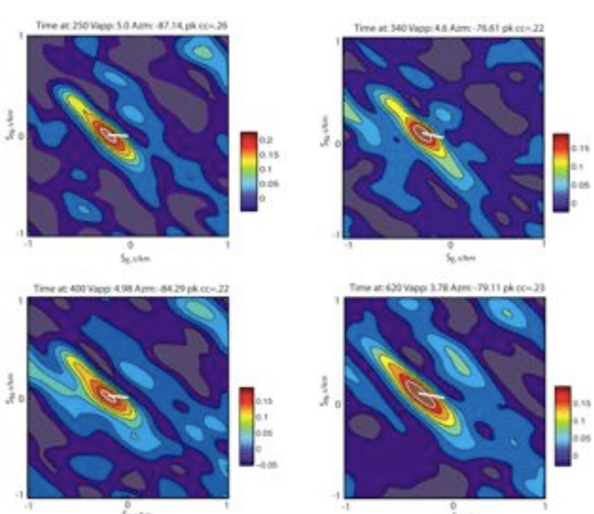

Azimuth and apparent velocity for the tremor event versus time determined for moving 20 s windows progressively shifted 10 s.

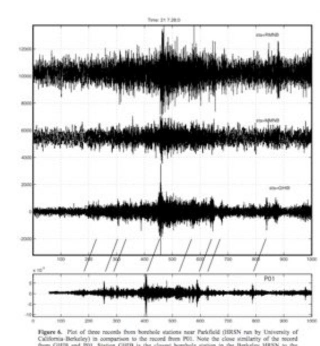

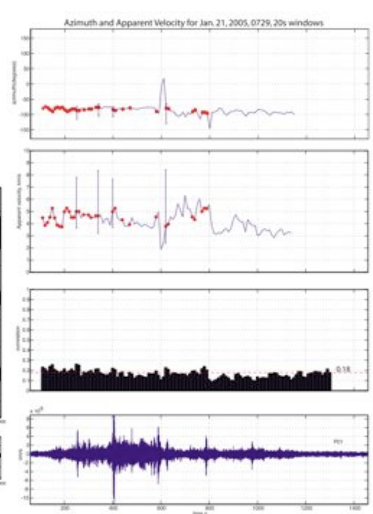

Tremor along the San Andreas Fault using a multiple array source imaging technique (Ryberg et al., GJI, 2010)

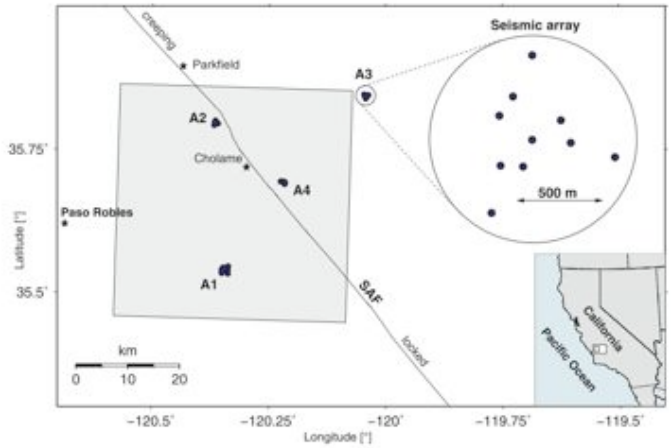

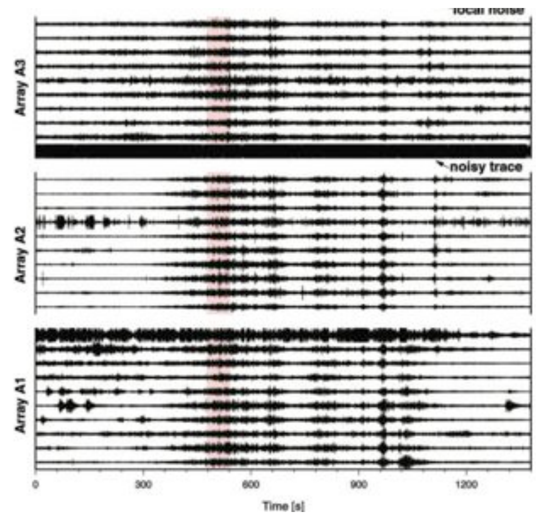

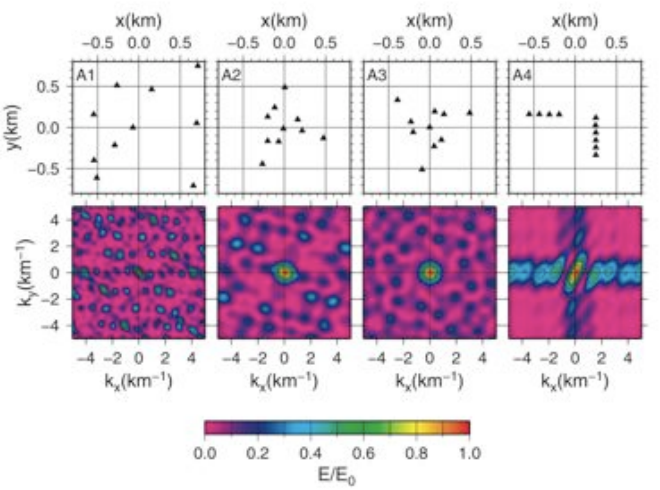

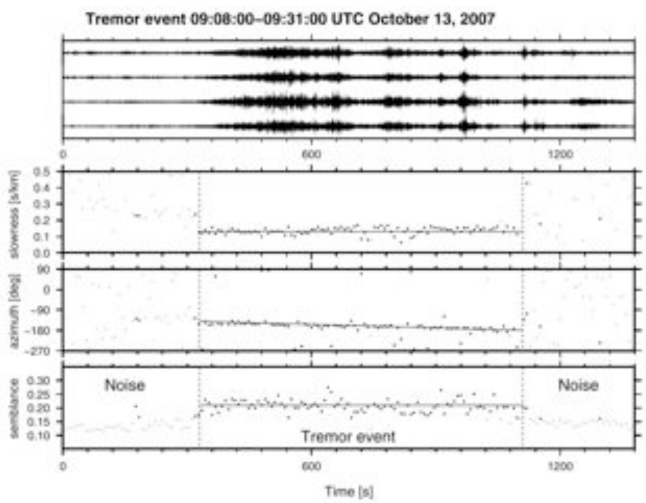

USGS Parkfield Dense Seismic Array (UPSAR) near the Parkfield section of the San Andreas Fault in Central California (Fletcher et al., BSSA, 2006)

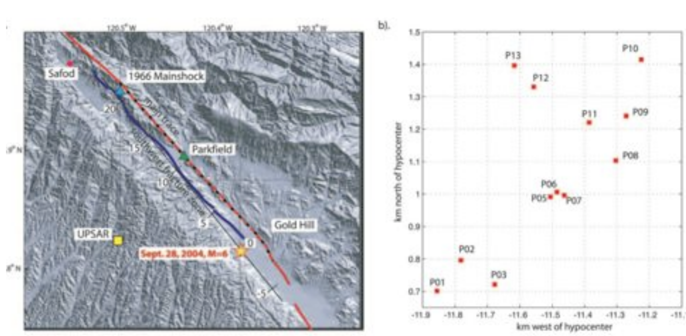

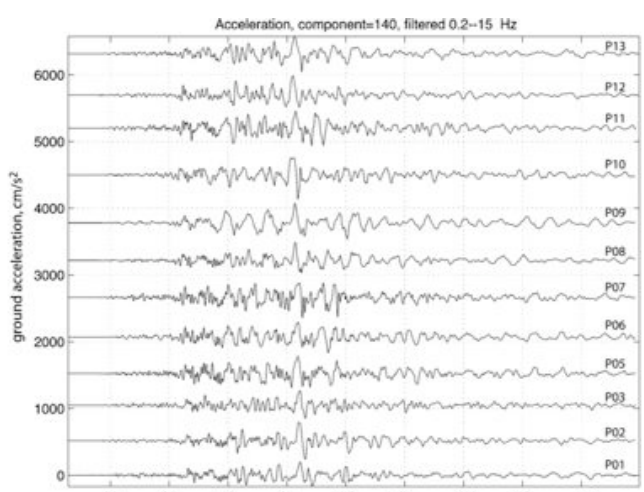

−0.7 to 0.7, in 0.01 sec/km increments. The time lag for a pair of stations is given by:

$$t_{ij} = s \cdot \mathbf{r}_{ij} + \delta t_i + \delta t_j,$$

$$\tau_{ij} = s \cdot r_{ij} + \delta t_i - \delta t_j$$

where $\mathbf{r}_{ij}$ is the vector pointing from station j to i, δt_i is the site delay determined for station i, $s = (s_E, s_N, s_Z)$ is slowness, s_E and s_N are the slowness component in the east and north directions, respectively, and $s_Z = \sqrt{1/c^2 - s_E^2 - s_N^2}$, where c is the surface shear velocity obtained during the determination of site delays.

Correlation is then calculated by averaging

$$cc_{ij} = \left[\frac{\sum_t x_i(t)\, x_j(t - \tau_{ij})}{\sum_t x_i^2 \sum_t x_j^2}\right]^{1/2} \quad (1)$$

sqrt only to denominators

The azimuth and apparent velocity (c_{app}) corresponding to a given slowness vector are

$$az = \tan^{-1}\left(\frac{s_E}{s_N}\right), \quad (2)$$

and

$$c_{app} = \frac{1}{(s_E^2 + s_N^2)^{1/2}}. \quad (3)$$

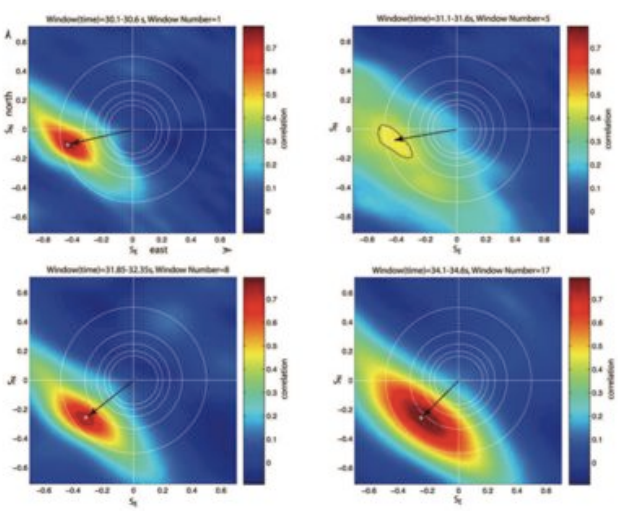

How to do array processing by yourself

1. **Write your own matlab script (part of homework 3).**
2. **Use an existing software package called GAP (Generic Array Processing) written by Prof. Keith Koper (SLU, now at Univ. Utah)**
3. Source code and example http://geophysics.eas.gatech.edu/people/zpeng/Software/GAP_koper_linux_all.tar.gz
4. Manual http://geophysics.eas.gatech.edu/people/zpeng/Software/GAP_manual.pdf

Infrasound arrays at infrasound monitoring station in Qaanaaq, Greenland.

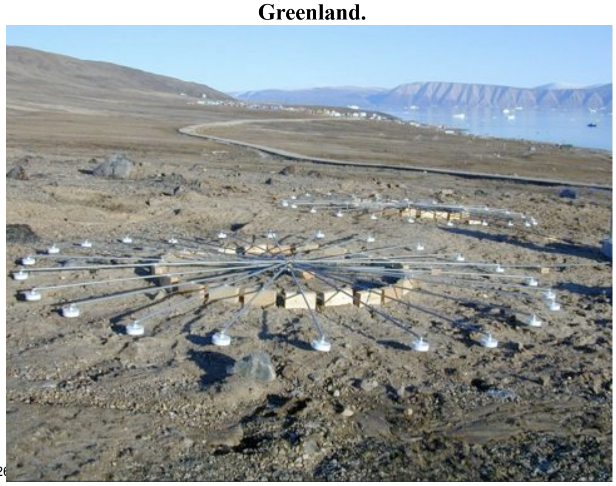

Infrasound, sometimes referred to as low-frequency sound, is sound that is lower in frequency than 20 Hz (Hertz) or cycles per second, the "normal" limit of human hearing.

Infrasound sometimes results naturally from severe weather, surf,[6] lee waves, avalanches, earthquakes, volcanoes, bolides,[7] waterfalls, calving of icebergs, aurorae, lightning and upper-atmospheric lightning.[8] Nonlinear ocean wave interactions in ocean storms produce pervasive infrasound vibrations around 0.2 Hz, known as microbaroms.[9] According to the Infrasonics Program at the NOAA, infrasonic arrays can be used to locate avalanches in the Rocky Mountains, and to detect tornadoes on the high plains several minutes before they touch down.[10]

Infrasound also can be generated by human-made processes such as sonic booms and explosions (both chemical and nuclear), by machinery such as diesel engines and older designs of down tower wind turbines and by specially designed mechanical transducers (industrial vibration tables) and large-scale subwoofer loudspeakers [11] such as rotary woofers. The Comprehensive Nuclear-Test-Ban Treaty Organization Preparatory Commission uses infrasound as one of its monitoring technologies (along with seismic, hydroacoustic, and atmospheric radionuclide monitoring).

An infrasound array study of Mount St. Helens (Matoza et al., JVGR, 2007)

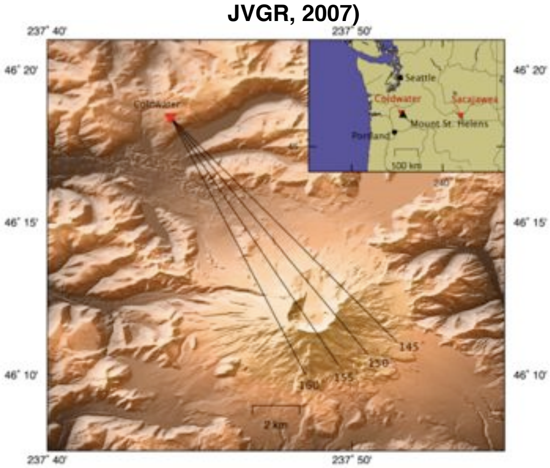

Comparisons between the seismic and infrasound recording of the drumbeat earthquakes

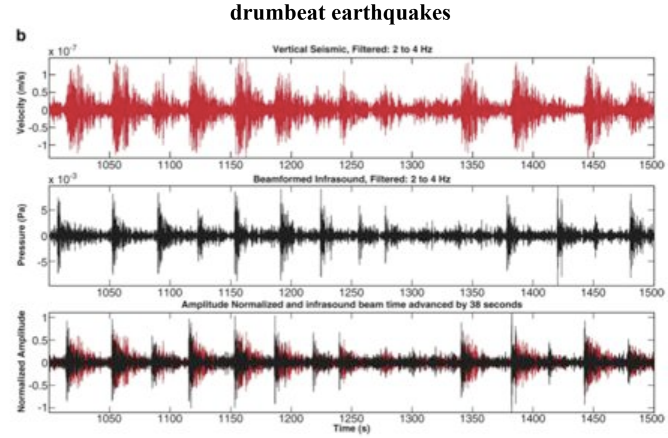

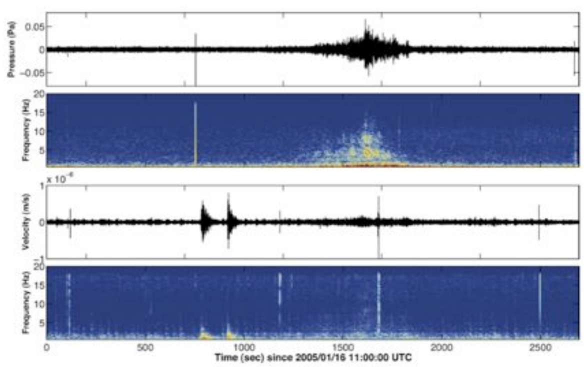

Fig. 5. Infrasound beam and its corresponding spectrogram (upper two panels), compared to the co-located vertical seismic channel and corresponding spectrogram (lower two panels) for the January 16th, 2005 eruption observed at Coldwater. The time series data are shown filtered 1–10 Hz. The eruption is distinguished by a clear infrasonic signal between ~ 1300 s and ~ 1800 s. The eruption is preceded ~ 500 s prior by two seismic LP events without infrasonic twins. No significant seismicity is associated with the eruption.

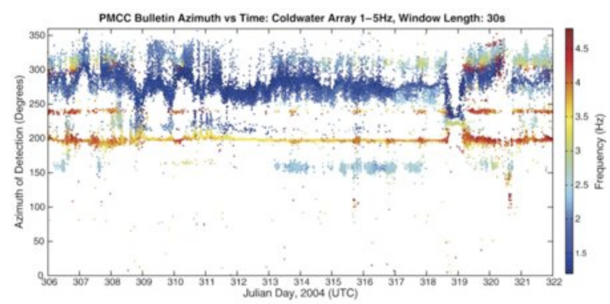

Fig. 3. Summary of PMCC detections at the Coldwater array, showing the arrival azimuth and frequency content (color) of coherent infrasound signals between Nov 1st and 16th, 2004 in the band 1–5 Hz. The continuous stream of high frequency (3.5–5 Hz — red dots) infrasound detections at ~ 200° and ~ 240° point directly at the nearby settlements of Portland (OR) and Kelso/Longview (WA). The lower frequency (1 Hz — dark blue dots) detections from a distributed source to the West (between 250° and 360°) point towards the Pacific Ocean. The bursts of 2–3 Hz detections at ~ 153° (especially between JD 313 and 318), turned out to be swarms of LP signals from Mount St. Helens. Plots like this give an overall picture of the characteristics of all of the separate infrasound sources recorded by the array at a given time, allowing one to identify signals of interest for detailed data analysis.

This Time

- Data management and basic data processing tools
- Systematic and random errors
- Waveform stacking
- Array analysis

- Further reading lists:
  - Rost, S., and C. Thomas (2002), Array seismology: Methods and applications, Rev. Geophys., 40(3), 1008, doi:10.1029/2000RG000100.
  - http://geophysics.eas.gatech.edu/internal/papers/2002/Rost/Rost_Thomas_RG_2002.pdf
  - S. Rost and E.J. Garnero (2004), Array seismology advances Earth interior research, EOS, 85, 301, 305-306.
  - http://geophysics.eas.gatech.edu/internal/papers/2004/Rost/Rost_Garnero_EOS_2004.pdf